

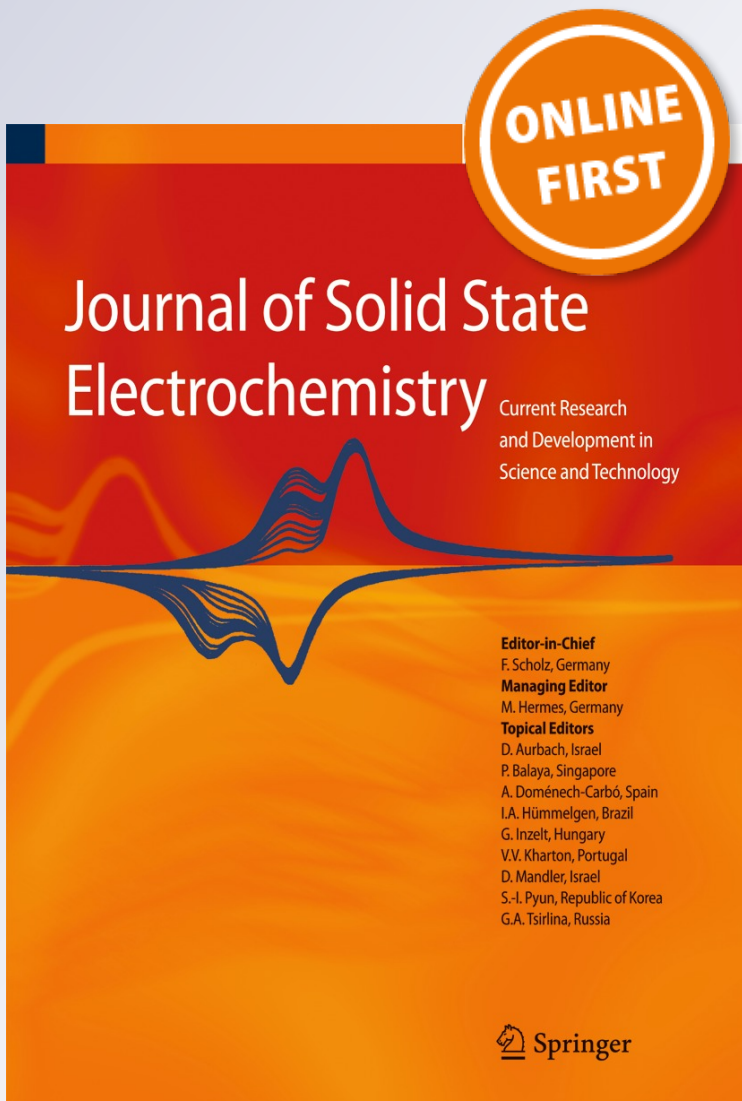
Stripping voltammetry method for determination of manganese as complex with oxine at the carbon paste electrode with and without modification with montmorillonite clay

Hanaa S. El-Desoky, Iqbal M. Ismail & Mohamed M. Ghoneim

Journal of Solid State Electrochemistry
Current Research and Development in Science and Technology

ISSN 1432-8488

J Solid State Electrochem
DOI 10.1007/s10008-013-2204-2



Your article is protected by copyright and all rights are held exclusively by Springer-Verlag Berlin Heidelberg. This e-offprint is for personal use only and shall not be self-archived in electronic repositories. If you wish to self-archive your article, please use the accepted manuscript version for posting on your own website. You may further deposit the accepted manuscript version in any repository, provided it is only made publicly available 12 months after official publication or later and provided acknowledgement is given to the original source of publication and a link is inserted to the published article on Springer's website. The link must be accompanied by the following text: "The final publication is available at link.springer.com".

Stripping voltammetry method for determination of manganese as complex with oxine at the carbon paste electrode with and without modification with montmorillonite clay

Hanaa S. El-Desoky · Iqbal M. Ismail ·
 Mohamed M. Ghoneim

Received: 6 June 2013 / Revised: 17 July 2013 / Accepted: 28 July 2013
 © Springer-Verlag Berlin Heidelberg 2013

Abstract Oxine (8-hydroxyquinoline) was used as an efficient and selective ligand for stripping voltammetry trace determination of Mn(II). A validated square-wave adsorptive cathodic stripping voltammetry method has been developed for determination of Mn(II) selectively as oxine complex using both the bare carbon paste electrode (CPE) and the modified CPE with 7 % (w/w) montmorillonite-Na clay. Modification of carbon paste with montmorillonite clay was found to greatly enhance its adsorption capacity. Limits of detection of 45 ng L^{-1} ($8.19 \times 10^{-10} \text{ mol L}^{-1}$) and 1.8 ng L^{-1} ($3.28 \times 10^{-11} \text{ mol L}^{-1}$) Mn(II) were achieved using the bare and modified CP electrodes, respectively. The achieved limits of detection of Mn(II) as oxine complex using the modified CPE are much sensitive than the detection limits obtained by most of the reported electrochemical methods. The developed stripping voltammetry method using both electrodes was successfully applied for trace determination of Mn(II) in various water samples without interferences from various organic and inorganic species.

Keywords Manganese · Oxine · CPE · Montmorillonite-Na clay · Determination · Stripping voltammetry

H. S. El-Desoky · M. M. Ghoneim (✉)
 Analytical and Electrochemistry Research Unit, Chemistry
 Department, Faculty of Science, Tanta University,
 31527 Tanta, Egypt
 e-mail: mmghoneim@usa.net

I. M. Ismail
 Department of Chemistry, Faculty of Science, and Center of
 Excellence in Environmental Studies, King Abdul Aziz University,
 21589 Jeddah, Saudi Arabia

Introduction

The rapid diffusion of heavy metals as environmental contaminants has called attention to their determination at trace and ultratrace levels. Manganese is considered to be the 12th most abundant element in the biosphere [1]. It is widely distributed in soil, sediment, water and in biological materials. Manganese is essential for normal development and body function across the life span of all mammals with some 20 identified functions in enzymes and proteins. Manganese contributes to maintain healthy nerves and immune system and helps in blood sugar regulation. It is involved in utilization of vitamins B₁ and E and required for normal bone growth or for avoiding blood clotting defects [2–4]. It is also essential for normal bone structure and the formation mucopolysaccharides [3]. Although manganese is essential for humans and other species of the animal kingdom as well as for plants, it is toxic at higher levels. In man, chronic manganese excess affects the central nervous system, with the symptoms resembling those of Parkinson's disease [4]. Relatively high doses of manganese affect DNA replication and causes mutations in microorganism and mammalian cells. In mammalian cells, manganese causes DNA damage and chromosome aberrations. Large amounts of manganese affect fertility in mammals and are toxic to the embryo and fetus [4].

Several analytical methods for Mn(II) determination have been reported in the literature, including spectrofluorimetry [5] spectrophotometry [6–10], flame atomic absorption spectrometry (FAAS), graphite furnace atomic absorption spectrometry (GFAAS), inductively coupled plasma-optical emission spectrometry (ICP-OES) [11–21], ion-selective electrodes [22, 23], and voltammetry [24–43]. In routine analysis, spectrophotometric methods are versatile and economical [6–10], but some of them are not sensitive enough (limit of detection [$\text{LOD} = 1.03 \times 10^{-7} \text{--} 2.02 \times 10^{-6} \text{ mol L}^{-1}$] [6–8] for

trace determination of Mn(II). Moreover, they are generally time-consuming and cannot be directly applied to manganese determination in seawater because of possible interferences caused by organic substances and variations in salinity. On the other hand, most of FAAS, GFAAS and ICP-OES methods [11–21] for the determination of trace concentrations of metal ions in high saline samples suffer also from matrix interferences [21] and required samples pretreatment [14–18]. Furthermore, although the ion-selective electrode methods [22, 23] are relatively simple, easy to handle and cheaper to design, their detection limits are also not sensitive enough for trace determination of Mn(II) ($\text{LOD}=5.46\times10^{-8}\text{--}3.99\times10^{-7}\text{ mol L}^{-1}$).

Because of the widespread use of voltammetry in the determination of Mn(II), comparison between the existing voltammetric methods [24–44] is shown in Table 1. It was

shown that the detection limit of determination of Mn(II) at the dropping mercury electrode (DME) by the differential pulse polarography (DPP) [24] is relatively high ($\text{LOD}=9.1\times10^{-8}\text{ mol L}^{-1}$). Moreover, the electrocatalytic reduction of Mn(II) at the $\text{C}_{60}/\text{Li}^+$ modified GC electrode using cyclic voltammetry [25] is also not sensitive enough for its determination ($\text{LOD}=9.19\times10^{-6}\text{ mol L}^{-1}$), and other heavy metal ions such as Hg(II), Cd(II) and Cu(II) appeared to exert a positive interference on the reduction peaks of Mn(II). However, the lithium-doped modified indium tin oxide (ITO) electrode was proven to be sensitive towards the detection of Mn(II) ($\text{LOD}=1.0\times10^{-9}\text{ mol L}^{-1}$) using cyclic voltammetry [26]; nevertheless, this work suffered from lack of validation of the method, which is relatively costly because of the electrode disposable material.

Table 1 Comparison of the detection limits and the experimental conditions of the various reported electrochemical methods to those of the described methods for Mn(II) determination as oxine complex

Electrode	Medium	Technique	LOD (mol L ⁻¹)	Ref.
DME	Citrate–borate solution (pH 9.5)	DPP	9.10×10^{-8}	[24]
$\text{C}_{60}/\text{Li}^+$ modified GC electrode	0.1 mol L ⁻¹ KCl	CV	9.19×10^{-6}	[25]
Lithium doped modified Indium Tin oxide (ITO) electrode	0.1 mol L ⁻¹ KCl	CV	1.00×10^{-9}	[26]
Chemically modified bentonite–porphyrin carbon paste electrode (MBPCE)	Universal buffer (pH 6.5)	CV-ASV	1.00×10^{-7}	[27]
MFE	0.01 mol L ⁻¹ borate buffer (pH 8.6)	DP-ASV	2.91×10^{-10}	[28]
HMDE	$\text{NH}_3/\text{NH}_4\text{Cl}$ (pH 9)	DP-ASV	8.37×10^{-10}	[29]
Stationary mercury electrode	$\text{NH}_3/\text{NH}_4\text{Cl}$ (pH 9)	DP-ASV and DP-CSV	1.00×10^{-9}	[30]
Metal catalyst free carbon nanotube (MCFCNT)	0.05 mol L ⁻¹ NH_4Cl (pH 3)	SW-ASV	1.20×10^{-7}	[31]
Metal catalyst free carbon nanotube (MCFCNT)	0.1 mol L ⁻¹ borate buffer (pH 8.5)	SW-CSV	9.30×10^{-8}	[31]
GCE	0.04 mol L ⁻¹ $\text{NH}_3/\text{NH}_4\text{Cl}$ (pH 9)	LS-CSV	1.00×10^{-9}	[32]
Graphite based polymer composite electrode	Acetate ammonium buffer (pH 9)	SW-CSV	3.64×10^{-9}	[33]
Boron-doped diamond electrode	Ammonium nitrate (pH 7)	DP-CSV	1.00×10^{-11}	[34]
A carbon paste electrode modified with 1-(2-pyridylazo)-2-naphthol	Phosphate–borax buffer (pH 8.7)	DP-CSV	6.91×10^{-9}	[35]
A mercury-free thick-film graphite-containing electrode modified with formazan	0.1 mol L ⁻¹ NaCl + ammonia buffer (pH 9.2)	DP-CSV	7.28×10^{-10}	[36]
Carbon film electrodes	0.2 mol L ⁻¹ H_3BO_3 /0.1 mol L ⁻¹ KCl (pH 7.2)	SW-CSV	4.00×10^{-9}	[37]
CPE	0.1 mol L ⁻¹ phosphate buffer (pH 7.4)	DP-CSV	1.00×10^{-7}	[38]
HMDE	$\text{NH}_3/\text{NH}_4\text{Cl}$	DP-AdCSV	4.00×10^{-10}	[39]
HMDE	0.01 mol L ⁻¹ ammonia buffer (pH 8.8) + 5-Br-PADAP	DP-AdCSV	3.64×10^{-9}	[40]
GCE	0.05 mol L ⁻¹ acetic acid/ NH_4OH (pH 9)	SW-AdCSV	4.00×10^{-10}	[41]
CPE	0.1 mol L ⁻¹ acetate buffer (pH 5)+5-Br-PADAP	SW-AdCSV	1.20×10^{-9}	[42]
CPE modified with 10 % montmorillonite clay	0.1 mol L ⁻¹ acetate buffer (pH 5) + 5-Br-PADAP	SW-AdCSV	2.73×10^{-10}	[43]
CPE	0.1 mol L ⁻¹ acetate buffer (pH 5)+oxine	SW-AdCSV	8.19×10^{-10}	Present work
CPE modified with 7 % (w/w) montmorillonite-Na clay	0.1 mol L ⁻¹ acetate buffer (pH 5)+oxine	SW-AdCSV	3.28×10^{-11}	Present work

Anodic stripping voltammetry (ASV) has been used for determination of Mn(II) using various kinds of working electrodes [27–31]. However, determination of trace manganese by ASV using the mercury electrodes [28–30] suffer from three problems: (1) the low solubility of manganese in mercury, (2) the deposition potential of Mn(II) was close to the discharge potential of hydrogen ions (-1.7 V vs. SCE), and (3) formation of intermetallic compounds at the mercury electrode [30]. Since the reduction potential of Mn(II) was beyond the potential range of most of the common solid electrodes, most of the reported ASV methods for determination of Mn(II) were conducted at Hg electrodes [28–30]. Due to toxicity concerns, the use of Hg is often limited, making these analyses unsuitable for many applications.

On the other hand, traces of manganese have been determined by cathodic stripping voltammetry (CSV) using various solid electrodes (carbon, modified carbon paste, carbon film, glassy carbon and boron-doped diamond) [30–38]. The determination of Mn(II) by CSV involves electrolytic preconcentration step where the trace Mn(II) is oxidized to Mn(IV). Mn(IV) immediately hydrolyses to form manganese dioxide (or its hydrate) on the electrode surface $\{Mn^{+2}(H_2O)_x(aq) \rightarrow MnO_2(H_2O)_{x-y(s)} + (y-2)H_2O + 4H^+ + 2e^- \}$ depending on the pH of the medium and the oxidative deposition applied potential [38]. The deposited MnO_2 was then reduced to Mn(II) in the determination step (stripping step) by negative potential scan. Since the solubility of MnO_2 is quite dependent on the pH of the solution, a basic medium is necessary for the formation of MnO_2 [30–33, 35, 36]. The more acidic solution makes formation of MnO_2 difficult [31]. The disadvantages of this method are that: (1) there is a tendency for incomplete precipitation of insoluble dioxide and (2) the method has a narrow working concentration range and poor selectivity. CSV method has significant interfering of cations, e.g., Zn(II) (it may destroy the active site of the pretreated electrode) [32], Tl(II) [33], Al(III) [34], Fe(II) [34–37], Ni(II) [37], Co(II) [32, 35], Hg(II) [34, 35], Cu(II) (copper interference by reduction peak of Cu(II) at -0.04 V versus SCE masking the MnO_2 peak) [37], and Pb(II) (Pb(II) is easily oxidized to PbO_2 , which can be co-deposited onto the electrode surface together with MnO_2) [33, 37].

In order to eliminate the limitations of ASV and CSV for manganese determination, an organic ligand is used to complex Mn(II); this complex has an adsorptive property rather than an electrolytic accumulation onto the surface of the electrode [39–43]. Adsorptive stripping voltammetry (AdSV) approach is based on adsorptive accumulation (non-electrolytic) of the analyte onto the electrode surface under open circuit conditions (where no charge transferred). AdSV methods have been reported for the determination of manganese as metal complexes with different ligands at the hanging mercury drop [39, 40], glass carbon [41] and carbon paste [42, 43] electrodes. The achieved LOD of Mn(II) as metal

complexes by these methods at some solid and mercury electrodes were 2.73×10^{-10} to 3.64×10^{-9} mol L $^{-1}$.

Oxine (8-hydroxyquinoline) is a bidentate chelating agent [44] capable of forming complexes with several metal ions. However, no adsorptive CSV method is reported in literature yet for determination of Mn(II) as oxine complex. On the other hand, mixing the carbon paste with some sort of adsorptive species (modifier) notably increases the sensitivity of the CPE towards determination of analytes. The different approaches that have been taken in the development of electrochemical sensors incorporating carbon as the principal electrode substrate were reviewed [45]. Montmorillonite-Na (MMT-Na) clay belongs to the smectite group of clays with a layer lattice (Fig. 1). Because of its high chemical and mechanical stability, well-layered structure and strong adsorptive properties (which are attributed to the expandability of its internal layers), it has been used in this work as a modifier. This work aimed to describe a simple and precise square-wave adsorptive CSV method for trace determination of Mn(II) as oxine complex in water samples using both the bare carbon paste electrode (CPE) and the developed CPE modified with MMT-Na clay.

Experimental

Solutions and apparatus

A 1×10^{-3} mol L $^{-1}$ 8-hydroxyquinoline (oxine) solution was prepared by dissolving an appropriate amount of the compound (Merck) in spec-pure methanol. Desired standard solutions of K(I), Na(I), Mg(II), Ca(II), Al(III), Cu(II), Cd(II), Pb(II), Sb(III), Bi(III), Se(IV), Zn(II), Mn(II), V(V), Ti(IV), Ni(II), Co(II) and Fe(III) were prepared by accurate dilution of their standard stock solutions (1,000 mg L $^{-1}$ dissolved in aqueous 0.10 mol L $^{-1}$ HCl, supplied from Cica, Japan) by de-ionized water. Solutions (1,000 mg L $^{-1}$) of each of HCO_3^- , Cl^- , NO_3^- , SO_4^{2-} and PO_4^{3-} were prepared by dissolving appropriate amounts of $NaHCO_3$, KCl , KNO_3 , Na_2SO_4 and Na_3PO_4 , respectively, in de-ionized water. Next, 1,000 mg L $^{-1}$

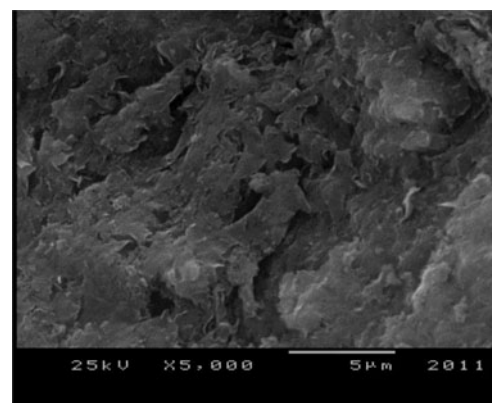


Fig. 1 SEM image of the montmorillonite (MMT-Na) clay surface

humic acid and 1 % Triton X-100 solutions were prepared in de-ionized water.

Britton–Robinson (B-R) universal buffer (pH 2–11), acetate buffer (pH 3.75–5.75) and phosphate buffer (pH 3–8) as supporting electrolytes were prepared in de-ionized water. All chemicals used were of analytical-grade reagents and were used without further purification. The de-ionized water used throughout the present work was obtained from a Purite-Still Plus Deionizer connected to a Hamilton-Aqua Matic bi-distillation water system (Hamilton Laboratory Glass Ltd, Kent, UK).

Computer-controlled Potentiostats Models 263A and 273A (Princeton Applied Research, Oak Ridge, TN, USA) with the software 270/250-PAR were used for the voltammetric measurements. A micro-electrolysis cell consisting of C-2 stand with electrode body (BASi Model MF-2010), an Ag/AgCl/KCl_s reference electrode (BASi Model MF-2079), and a platinum wire counter electrode was used. A magnetic stirrer with a Teflon-coated magnet was used to provide the convective transport during the preconcentration step. Electrode assembly (Model 303A-PAR) incorporating a micro-electrolysis cell of a three electrode system comprising of a hanging mercury drop electrode (HMDE) as a working electrode (area: 0.026 cm²), an Ag/AgCl/KCl_s reference electrode and a platinum wire counter electrode, was also used.

Preparation of the bare and modified carbon paste electrodes

The carbon paste was fabricated by mixing an amount (5 g) of graphite powder (1–2 µm, Aldrich, Milwaukee, WI, USA) and 1.8 ml Nujol oil (Sigma, $d=0.84 \text{ g l}^{-1}$) uniformly by milling in a small agate mortar, whereas CPE modified with 1–11 % (wt/wt) MMT-Na clay were fabricated by mixing an amount (4.95–4.45 g) of graphite powder and (0.05–0.55 g) of MMT-Na clay (fine powder <5 µm; ECC America Inc., Southern Clay Products Subsidiary, Gonzales, TX, USA) uniformly by milling in a small agate mortar. Then, 1.8–2.0 ml Nujol oil was added and milled again to give a homogenous paste. The body of the electrode was a Teflon rod with end cavity (BASi Model MF-2010, 3 mm diameter and 1 mm deep) bored at one end for paste filling. Contact was made with a copper wire through the centre of the Teflon rod. An amount of the fabricated carbon paste or that modified with MMT-Na clay was pressed into the end cavity of the electrode body and leveled off with a spatula. The surface of the fabricated bare CPE and the modified one was manually smoothed by polishing on a clean paper before use. JEOL JSM 5400 scanning electron microscopy (SEM) was used to observe the surface morphology of the carbon paste (CP), MMT-Na clay, and the modified CP with various ratios of MMT-Na clay. The discs of samples used for morphology examination were prepared by pressing the materials. The pressed specimens were then fractured and the fracture surface was sputtered with gold prior to observation.

Analyzed environmental water samples

Various water samples such as: groundwater, tap water, bottled natural water (available in the Egyptian market) and coastal seawater (from coast of Alexandria City, Egypt) samples were analyzed. The seawater sample was taken a few meters from the coast where the water was 3–4 m deep. Then, the seawater sample was UV-digested (30 min) after acidification with HCl to pH 1 with a 1-kW high-pressure mercury vapor lamp to avoid possible interferences caused by natural organic compounds and to breakdown organic-metal complexes. Then, for 5 ml of each sample (with or without dilution by de-ionized water according to the concentration level of Mn(II) in its different water samples), 5 ml of the supporting electrolyte was added, and the analysis was performed by a developed square-wave adsorptive cathodic striping voltammetry (SW-AdCSV) method at both the CPE and the modified CPE with 7 % (w/w) MMT-Na clay.

Results and discussion

Electrochemical investigation of oxine and Mn(II)–oxine complex systems

Cyclic voltammograms of 50 µM oxine in 0.1 mol L⁻¹ acetate buffer of pH 5 recorded at both the bare CPE and the modified CPE with MMT-Na clay show two cathodic peaks (P_{1c}) and (P_{2c}) at +0.40 and −0.02 V and two corresponding anodic peaks (P_{1a}) and (P_{2a}) in the reverse scan at +0.57 and +0.15 V, in addition to a third irreversible anodic peak (P_{3a}) at very positive potential (+0.78 V) (Fig. 2, curves a and b).

The peak current magnitudes are much enhanced at the modified CPE (Fig. 2, curve b). The two cathodic peaks (P_{1c}) and (P_{2c}) may correspond to the reduction of the $-\text{C}=\text{N}-$ double bond of the pyridine ring [46] of the basic (HL) and the acidic (H_2L^+) forms of oxine, respectively ($\text{p}K_{\text{a}1} (= \text{NH}^+/-\text{N}-) = 5.03-5.11$, which is attributed to deprotonation of the basic nitrogen atom of its pyridine ring) [47] (Scheme 1). Meanwhile, the anodic peak (P_{3a}) (at +0.78 V) may correspond to two-electron irreversible oxidation of the acidic and/or the basic form of oxine [48]. The suggested electrode reaction of oxine at CP electrodes is illustrated in Scheme 1.

On the other hand, cyclic voltammogram of 100 µg l⁻¹ of Mn(II) in 0.1 M acetate buffer of pH 5 showed no voltammetric peaks within the potential range of the CPE and the modified one following preconcentration under open circuit conditions or by adsorptive accumulation at $E_{\text{acc}} = +1.20 \text{ V}$ for 250 s (e.g., Fig. 3a, curve a). However, a cyclic voltammogram of 100 µg l⁻¹ of Mn(II) in the presence of 50 µM oxine exhibited a new small cathodic peak (P_{4c}) at +0.65 V and a corresponding anodic one (P_{4a}) at +1.00 V in the

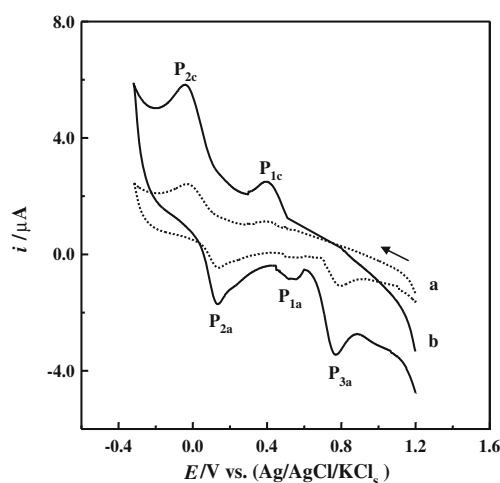
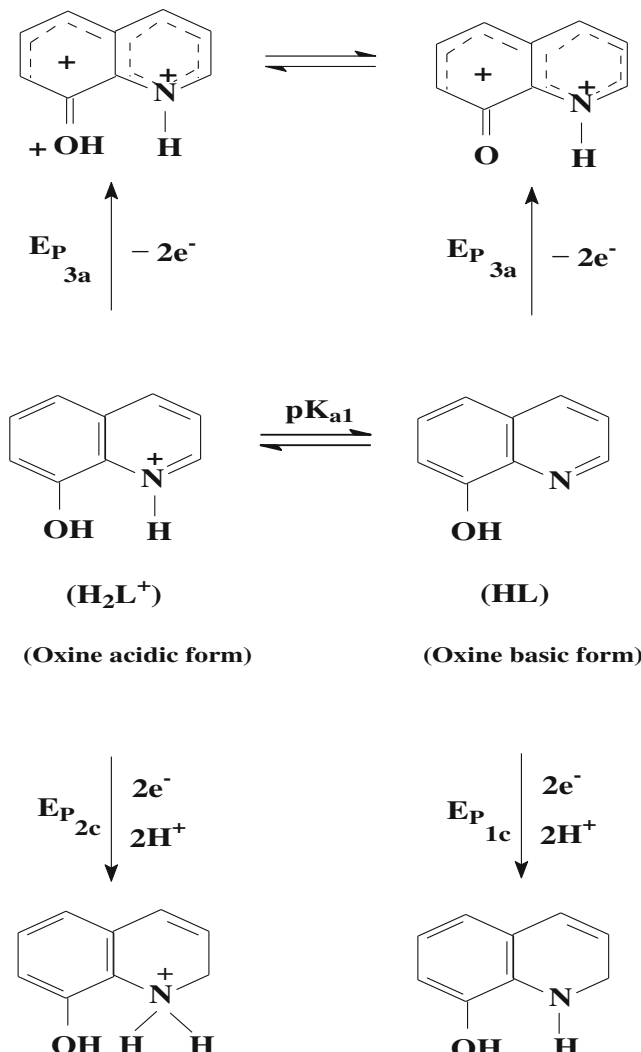


Fig. 2 Cyclic voltammograms recorded in 0.1 mol L⁻¹ acetate buffer of pH 5 for 50 μM oxine at the bare CPE (**a**) and the CPE modified with 7 % (w/w) MMT-Na clay (**b**); scan rate 200 mV s⁻¹



Scheme 1 The suggested electrode reaction mechanism of oxine at the carbon paste electrodes

reverse scan which attributed to the formed Mn(II)-oxine complex, (e.g., Fig. 3a, curve b, solid line).

The peak current magnitudes of the cathodic peak (P_{1c}) as well as of the anodic peaks (P_{1a}) and (P_{3a}) of oxine are decreased indicating the consumption of oxine in complex formation reaction, (e.g., Fig. 3a, curve b). However, following preconcentration onto the bare and the modified CP electrodes by adsorption accumulation at +1.20 V for 250 s, the cathodic peak (P_{1c}) and the anodic peak (P_{1a}) of the neutral form of oxine disappeared completely with an obvious

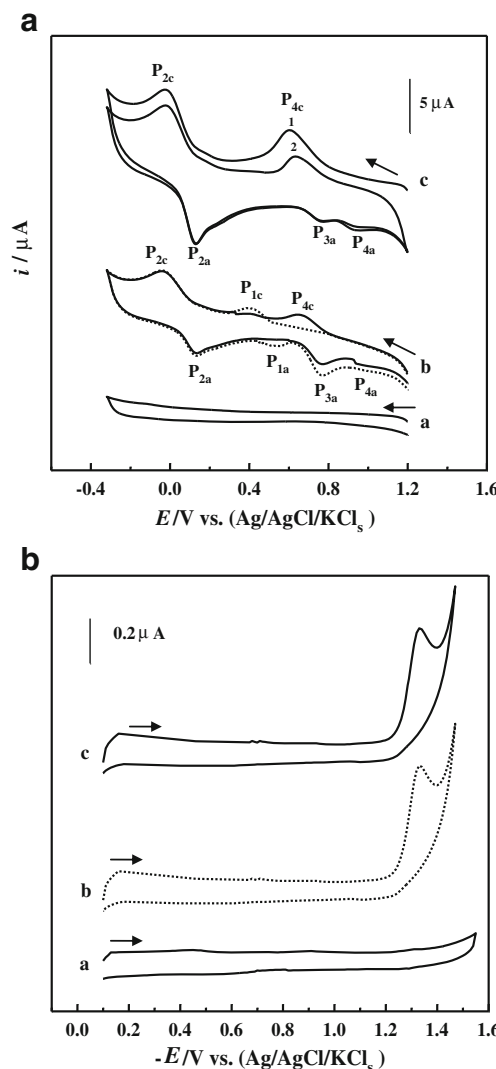
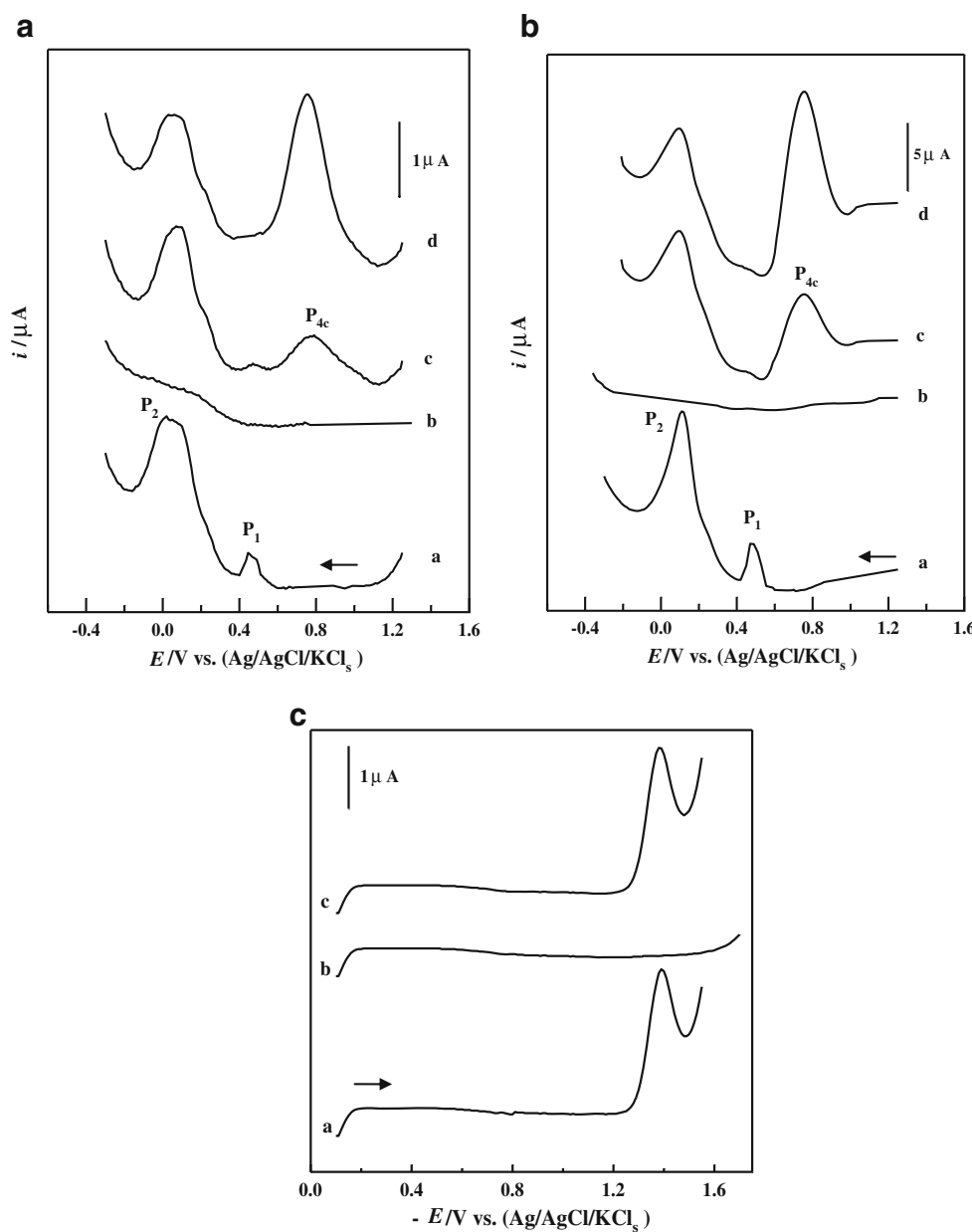


Fig. 3 **a** Cyclic voltammograms recorded in 0.1 mol L⁻¹ acetate buffer of pH 5 for (a) 100 μg L⁻¹ of Mn(II), (b and c) 100 μg L⁻¹ of Mn(II)+50 μM oxine following preconcentration under open circuit conditions onto the CPE modified with 7 % (w/w) MMT-Na clay (b) or by adsorptive accumulation for 250 s at $E_{acc}=+1.20$ V (a and c). 1 First cycle, 2-second cycle; scan rate=200 mVs⁻¹ (dotted curve is for oxine in the absence of Mn(II)). **b** Cyclic voltammograms recorded in 0.1 mol L⁻¹ acetate buffer of pH 5 for (a) 100 μg L⁻¹ of Mn(II), (b) 50 μM oxine and (c) 100 μg L⁻¹ of Mn(II)+50 μM oxine, following preconcentration onto HMDE by adsorptive accumulation for 100 s at $E_{acc}=-0.1$ V; scan rate 200 mV s⁻¹

Fig. 4 SW-AdCS voltammograms recorded in 0.1 mol L⁻¹ acetate buffer of pH 5 following preconcentration onto the bare CPE (**a**) and the CPE modified with 7 % (w/w) MMT-Na clay (**b**) by adsorptive accumulation for 50 s at +1.25 V for: (a) 30 μM oxine; (b) 10 μg l⁻¹ of each of Cd(II), Pb(II), Cu(II), Sb(III), Bi(III), Se(IV), Zn(II), Mn(II), Ni(II), Co(II), Fe(III), Al(III), V(V) and Ti(IV) in the absence of oxine; (c) a solution of (a + b); and (d) for the solution of (a + b) + additional 10 μg l⁻¹ of Mn(II); ($f=80$ Hz, $\Delta E_s=10$ mV and $E_a=25$ mV). (**c**) SW-AdCS voltammograms recorded in 0.1 mol L⁻¹ acetate buffer of pH 5 following preconcentration onto HMDE by adsorptive accumulation for 50 s at -0.1 V for: (a) 30 μM oxine, (b) 20 μg l⁻¹ of Mn(II) in the absence of oxine, and (c) 30 μM oxine+20 μg l⁻¹ of Mn(II); ($f=80$ Hz, $\Delta E_s=10$ mV and $E_a=25$ mV)



decrease in peak current magnitude of the oxidation peak (P_{3a}), (e.g., Fig. 3a, curve c, first cycle 1), indicating that this peak (P_{3a}) corresponds to the oxidation of the basic (neutral) form of oxine rather than its acidic (protonated) form. The basic form of oxine has much ability to contribute in Mn(II)-oxine complex formation. This behavior was also clearly observed upon increasing the concentration of Mn(II), the large enhancement of cathodic peak (P_{4c}) and its reversed anodic peak (P_{4c}) of Mn(II)-oxine complex with the complete disappearance of anodic peak (P_{3a}) of oxine, consequently confirming the formation of neutral Mn(II)-oxine complex (Scheme 1). Moreover, a better developed peak current of Mn-oxine complex (P_{4c}) was observed at the modified CPE (Fig. 3a, curve c; first cycle 1) compared to the bare one. This indicated a better adsorption of Mn(II)-oxine complex onto the

modified CPE. Moreover, a substantial decrease of the monitored voltammetric peak current of Mn(II)-oxine complex (P_{4c}) was observed in the second cycle 2 (Fig. 3a, curve c), indicating the desorption of Mn(II)-oxine complex from the electrode surface.

On the other side, the cyclic voltammogram recorded in 0.1 M acetate buffer of pH 5 for 100 μg l⁻¹ of Mn(II) following preconcentration under open circuit conditions or by adsorptive accumulation for 100 s at $E_{acc}=-0.1$ V onto the HMDE in the absence of oxine (e.g., Fig. 3b, curve a) exhibited no cathodic peak corresponding to the Mn(II) reduction. Meanwhile, the cyclic voltammogram of 50 μM oxine (e.g., Fig. 3b, curve b) exhibited a single cathodic peak around -1.32 V, which may correspond to the reduction of oxine. Moreover, the cyclic voltammogram of a solution of 100 μg l⁻¹ of Mn(II) in the

presence of 50 μM oxine exhibited no new cathodic peak that corresponds to the Mn(II)-oxine complex (Fig. 3b, curve c), i.e., Mn(II)-oxine complex did not respond at the HMDE, which may be due to the fact that Mn(II)-oxine complex has a very poor adsorptive character at the surface of HMDE compared to that at CP electrodes under the same experimental conditions, and/or the reduction potential of Mn(II)-oxine complex was beyond the potential range of mercury electrode.

Square wave investigation of oxine and metal-oxine complex systems

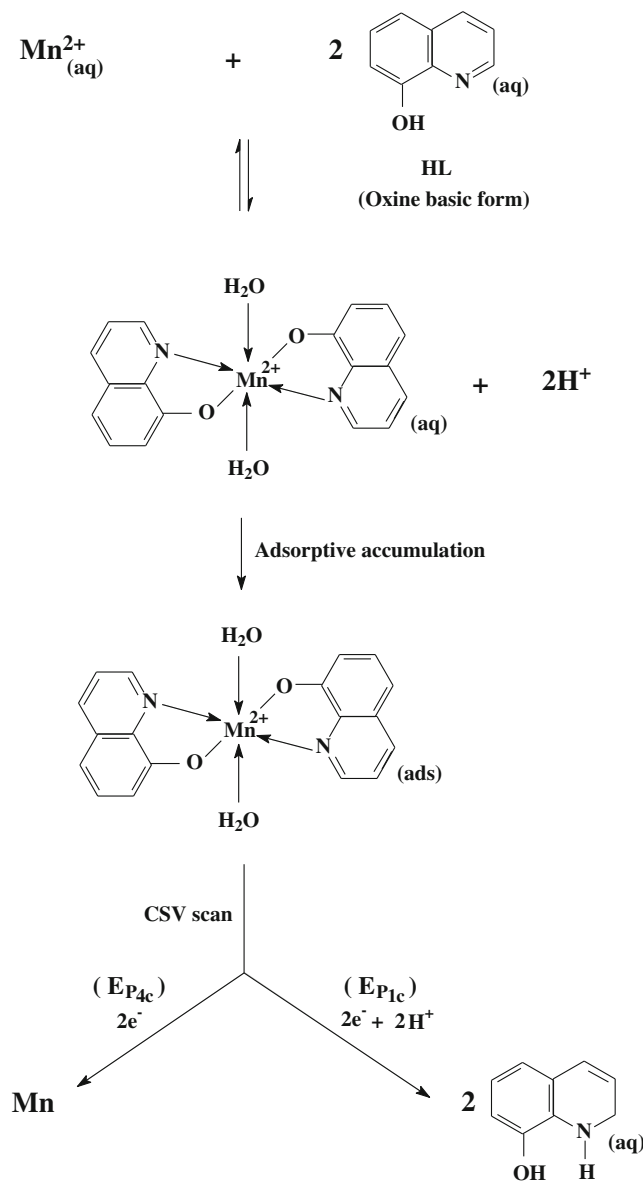
SW-AdCS voltammograms of solution of 30 μM oxine and (5–30) $\mu\text{g l}^{-1}$ Mn(II) were recorded by scanning the potential from +1.25 to −0.40 V (vs. Ag/AgCl/KCl_s) in 0.1 mol L^{−1} acetate buffer of pH 5 following preconcentration at both the bare CPE and the CPE modified with 7 % (wt/wt) MMT-Na clay by adsorption accumulation at +1.25 V for 50 s. The recorded voltammograms of oxine exhibited two cathodic peaks at +0.47 V (P_{1c}) and +0.09 V (P_{2c}), (Fig. 4a and b, curve a) corresponding to the reduction of the $-\text{C}=\text{N}-$ double bond of the pyridine ring [46] of the basic (HL) and the acidic (H_2L^+) forms of oxine, respectively.

On the other hand, SW-AdCS voltammogram of 0.1 mol L^{−1} acetate buffer of pH 5 containing 10 $\mu\text{g l}^{-1}$ of each of Mn(II), Cd(II), Pb(II), Cu(II), Sb(III), Bi(III), Se(IV), Zn(II), Ni(II), Co(II), Fe(III), Al(III), V(V) and Ti(IV) in the absence of oxine did not exhibit any voltammetric peaks (Fig. 4a and b, curve b). However, the voltammogram of this solution in the presence of 30 μM oxine exhibited a new well-defined cathodic peak (P_{4c}) at +0.8 V. The peak current magnitudes of P_{1c} of neutral oxine decreased, and that of the new peak (P_{4c}) increased with the addition of aliquots of Mn(II) (Fig. 4a and b, curves c and d), confirming again that P_{4c} corresponds to the reduction of the Mn(II)-oxine complex.

Moreover, no new cathodic peaks were observed upon the addition of different aliquots of each of Cd(II), Pb(II), Cu(II), Sb(III), Bi(III), Se(IV), Zn(II), Ni(II), Co(II), Fe(III), Al(III), V(V) and Ti(IV). This may be due to the very poor adsorptive character of their complexes onto the surface of both CP electrodes and/or non-complexing character of some of these metal ions with oxine under the experimental conditions. Moreover, the voltammetry peak of Mn(II)-oxine complex (P_{4c}) was found to respond perfectly to the extra addition of Mn(II) concentrations with the disappearance of the neutral oxine peak (P_{1c}), which clearly reflects again the formation of neutral Mn(II)-oxine complex. However, about 5-folds enhancement in peak current magnitude of Mn(II)-oxine complex was observed at the modified CPE (Fig. 4b, curves c and d) compared to that at the bare one (Fig. 4a, curves c and d), also confirming the strong adsorptive character of CPE modified with MMT-Na clay towards the Mn(II)-oxine complex.

As reported in the literature, the molar ratio of Mn(II) to oxine ligand in its complex was 1:2 [49]; thus, according to all the above results, the mechanism of formation and then reduction reaction of the Mn(II)-oxine complex following its preconcentration by adsorption accumulation onto both the CP electrodes can be suggested as follows:

- (1) The neutral Mn(II)-oxine complex formed first in the solution {the basic (neutral) form of oxine can greatly contribute in Mn(II)-oxine complex formation}.
- (2) Free oxine and Mn(II)-oxine complex were computationally preconcentrated by adsorptive accumulation onto the electrode surface at +1.25 V.



Scheme 2 Formation reaction of Mn(II)-oxine complex and its electrode reaction following its preconcentration by adsorption accumulation onto the carbon paste electrodes

- (3) Then, by scanning the potential cathodically from +1.25 to −0.4 V, both the accumulated Mn(II)–oxine complex and free oxine are reduced (stripping step) according to Schemes 2 and 1, respectively. P_{4c} corresponds to the reduction of Mn(II) in the accumulated complex, P_{1c} may correspond to the reduction of basic oxine in the accumulated complex and P_{2c} , and P_{2c} corresponds to the reduction of basic and acidic forms of the accumulated free oxine, respectively.

SW-AdCS voltammograms (e.g., Fig. 4c) indicated also that the Mn(II)–oxine complex did not respond at the HMDE even when various concentrations of Mn(II) and oxine were used and different accumulation potential and time were employed. Consequently, the cathodic peak (P_{4c}) at CP electrodes will be taken for quantitation of Mn(II) as Mn(II)–oxine complex in the rest of the analytical study.

Analytical studies

The interfacial accumulation of the Mn(II)–oxine complex at the CP electrodes surface can be used as an effective accumulation step to enhance the electroanalytical determination of Mn(II) using an optimized SW-AdCSV method

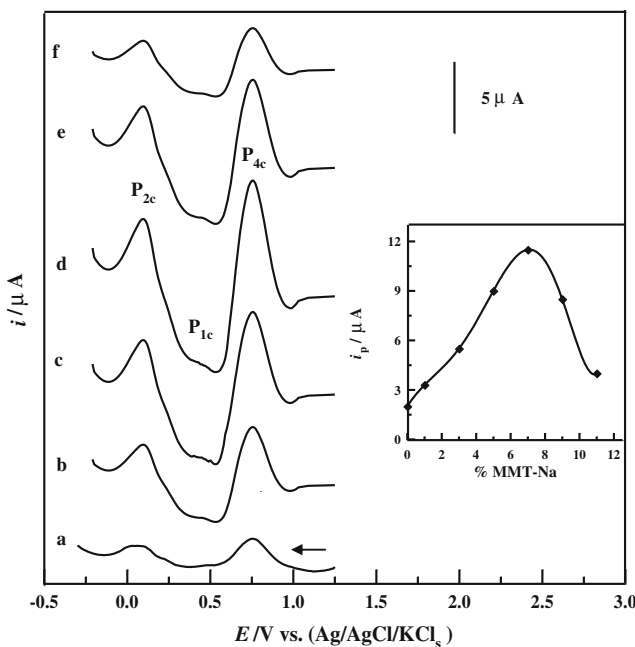


Fig. 5 SW-AdCS voltammograms recorded in 0.1 mol L⁻¹ acetate buffer of pH 5 for 20 µg L⁻¹ of Mn(II)+30 µM oxine, following preconcentration onto the bare CPE (a) and CPE modified with 3 % (b), 5 % (c), 7 % (d), 9 % (e) and 11 % (f) (w/w) MMT-Na clay by adsorptive accumulation for 50 s at +1.25 V. Inset: i_p as a function of % (w/w) MMT-Na clay; (f)=80 Hz, ΔE_s =10 mV and E_a =25 mV

Composition and stability of the modified CPE

The approach of mixing carbon paste with some sort of adsorptive species (modifier) notably increases the sensitivity of the CPE towards determination of analytes. In the present study, SW-AdCS voltammograms of 20 µg L⁻¹ of Mn(II) in the presence of 30 µM oxine were recorded in 0.1 mol L⁻¹ acetate buffer of pH 5 at CPE modified with various mass percentages (0–11 % w/w) of MMT-Na clay following preconcentration by adsorptive accumulation at +1.25 V (vs. Ag/AgCl/KCl_s) for 50 s. The peak current magnitude of Mn(II)–oxine complex increased upon the increase of mass percentage of MMT-Na clay in the modified CPE up to 7 % (w/w) (Fig. 5). At higher mass percentages of the clay in the modified CPE, the peak current magnitude decreased, which may be due to the decrease of conductivity in the modified

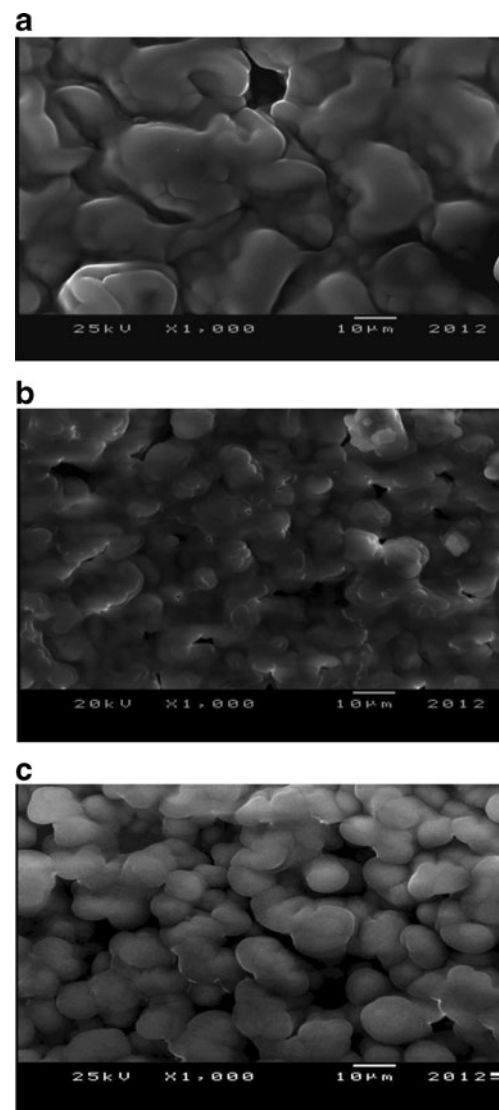


Fig. 6 SEM image of (a) CP, (b) CP modified with 5 %, and (c) CP modified with 7 % (w/w) MMT-Na clay

CPE, which hinders the electron transfer process and increases the background current and/or some change in its surface morphology. Therefore, a fabricated CPE modified with 7 % (w/w) MMT-Na clay was used for the rest of the analytical study in comparison with the bare CPE. On the other hand, an insignificant difference of peak current magnitude or its standard deviation (0.19–0.25) was noticed during the measurements over a week using the modified CP electrode, confirming that this electrode was stable and efficient towards the trace determination of Mn(II).

The strong interfacial adsorptive character of Mn(II)–oxine complex at the modified CPE under the optimum accumulation conditions can be attributed to the interesting morphological changes of its surface after modification with 7 % (w/w) MMT-Na clay compared to that of bare CPE and the other modified CPE with <7 % (w/w) MMT-Na clay. Scanning electron microscopy (SEM) was used to characterize the morphology of the bare CPE and carbon paste modified with 5 % and 7 % (w/w) MMT-Na clay (Fig. 6). The SEM image of the surface of bare carbon paste showed a microstructure with compact aggregates of large particles (Fig. 6a) while the surface of carbon paste modified with 5 % (w/w) MMT-Na was an ill-defined shaped structure of highly packed particles (Fig. 6b). However, significant differences in the structure of the carbon paste modified with 7 % (w/w) MMT-Na clay are observed (Fig. 6c). The main characteristic of 7 % (w/w) MMT-Na clay is the small particle size and the large surface area due to the discrete spherical particles morphology (the average diameter is $11.45 \pm 4.50 \mu\text{m}$) and numerous internal

holes. The increase in surface area for the sphere morphology resulted in enhancement of the voltammetric peak current as a consequence of the enhancement of sorption capacity of the modified CP with 7 % (w/w) MMT-Na clay compared to that of the bare CP or to that modified with 5 % (w/w) MMT-Na clay.

Effect of type of supporting electrolyte and its pH

The effect of supporting electrolyte and pH on the peak current magnitude of Mn(II)–oxine complex was studied for $20 \mu\text{g l}^{-1}$ of Mn(II) in the presence of $30 \mu\text{M}$ oxine in B-R universal buffer (pH 2–8), phosphate buffer (pH 5–8) and sodium acetate buffer (pH 3.75–5.75). The peak current magnitude increased with the increase in pH of the medium until it reached its maximum over the pH range 4.5–5.5, then decreased. The increase in the peak current magnitude as well as the shift in the peak potential to less positive values with increasing pH of the medium may be the result of increasing the formation and stability of the Mn(II)–oxine complex, respectively, due to the increase in the deprotonated (neutral) oxine [$\text{p}K_{\text{a}1} = \text{NH}^+/-\text{N}^- = 5.03-5.11$], which gave more adsorbed complexed species at the electrode surface. At pH values lower than 4.5, protonation of the nitrogen atom of the pyridine ring of oxine [47] can compete against the reaction between the Mn(II) and oxine. Therefore, Mn(II)–oxine complex formation rate is decreased (or dissociation of Mn–oxine complex is increased) and the yield of complex formation falls off and consequently the peak current magnitude decreased. In contrast, the obvious decrease in the peak current magnitude

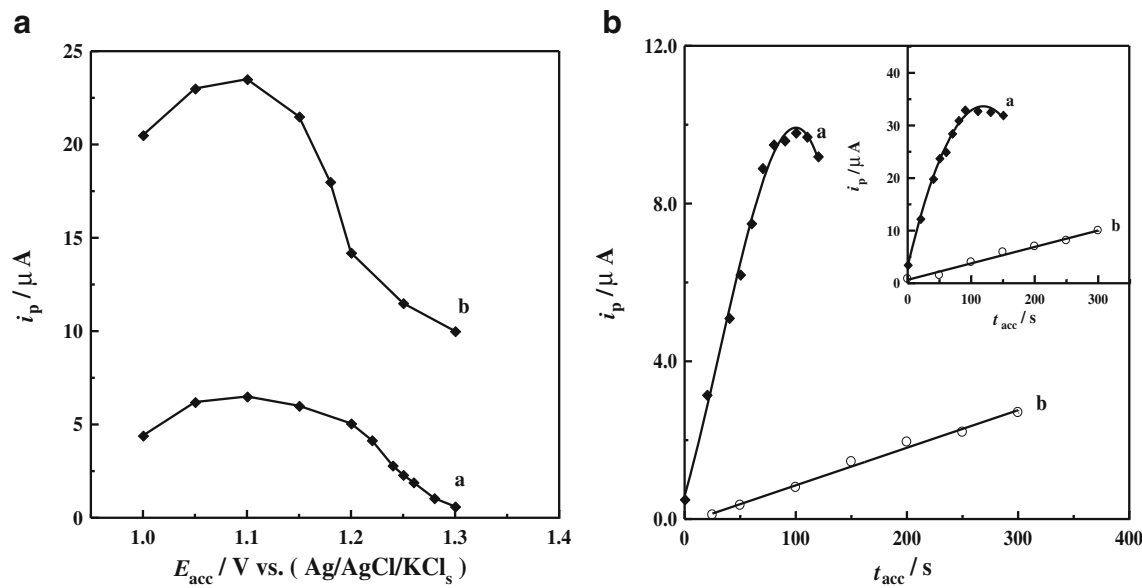


Fig. 7 **a** Plots of i_p versus E_{acc} for $20 \mu\text{g l}^{-1}$ Mn(II)+ $30 \mu\text{M}$ oxine following preconcentration by adsorptive accumulation for 50 s onto (a) the bare CPE and (b) the CPE modified with 7 % (w/w) MMT-Na clay. **b** Plots of i_p versus t_{acc} for (a) $20 \mu\text{g l}^{-1}$ and (b) $5 \mu\text{g l}^{-1}$ Mn(II)+ $30 \mu\text{M}$

oxine following preconcentration by adsorptive accumulation onto the bare CPE and the CPE modified with 7 % (w/w) MMT-Na clay (inset) at $+1.1 \text{ V}$ (in acetate buffer of pH 5; $f=80 \text{ Hz}$, $\Delta E_s=10 \text{ mV}$ and $E_a=25 \text{ mV}$)

at pH value above 6 may have been probably caused by precipitation of Mn(II) as Mn(II) oxinate precipitate $\{\text{Mn}(\text{C}_9\text{H}_6\text{ON})_2 \cdot 2\text{H}_2\text{O}\}$ [50], which affects the formation of Mn(II)-oxine complexes. Since sodium acetate buffer of pH 5 gave the best response using both bare CPE and modified CPE, it was chosen for subsequent experiments. This agrees well with a previous study, in which moderately acidic media (pH 4–5) were found to be the most suitable for the formation of metal-oxine complexes [51].

Effect of oxine ligand concentration

SW-AdCS voltammograms of $20 \mu\text{g l}^{-1}$ Mn(II) in acetate buffer of pH 5 were recorded in the presence of increasing concentrations of oxine (1 to $50 \mu\text{M}$) following preconcentration at bare CPE and CPE modified with 7 % (w/w) MMT-Na clay by adsorptive accumulation at +1.25 V for 50 s. The voltammograms showed that upon the increase of oxine concentration, enhancement of the peak current magnitude of the monitored SW-AdCSV signal was observed up to $10 \mu\text{M}$ oxine, and then remained constant until about $35 \mu\text{M}$ oxine, which may be due to the fact that the ligand does not compete with adsorption of the formed Mn(II)-oxine complex at the surface of the working electrode up to this concentration level. However, in the presence of oxine concentrations higher than $35 \mu\text{M}$, the peak current magnitude of Mn(II)-oxine complex decreased. This may be presumably caused by competitive adsorption of oxine at the working electrode surface with the complex. Accordingly, it seems that an oxine concentration of $10 \mu\text{M}$ might be adequate to ensure maximum stripping voltammetric response; hence, for further work this chelating agent concentration was selected.

On the other hand, the reaction kinetics of Mn(II) with oxine were identified from its voltammograms recorded after different mixing time of reactants. The peak current (i_p) magnitude of the examined Mn(II)-oxine complex was practically constant with the reaction time, indicating the immediate formation of Mn(II)-oxine complex within the mixing time of reactants in the electrochemical cell; therefore, heating of the reactants solution was not required in the present work.

Effect of pulse parameters

The response obtained by square-wave voltammetry is strongly dependent on pulse parameters such as frequency (f), pulse height (a) and scan increment (ΔE_s), which have a combined influence on the peak current magnitude. Hence, the influence of frequency f (10–120 Hz), scan increment ΔE_s (2–10 mV) and pulse-height a (5–35 mV) on the SW-AdCSV peak current magnitude of $20 \mu\text{g l}^{-1}$ of Mn(II) in acetate buffer of pH 5 in the presence of $10 \mu\text{M}$ oxine, following preconcentration onto the bare and modified CP electrodes at $E_{\text{acc}}=+1.25$ V for 50 s, was examined. A better developed and symmetrical voltammetric peak was obtained at the following pulse

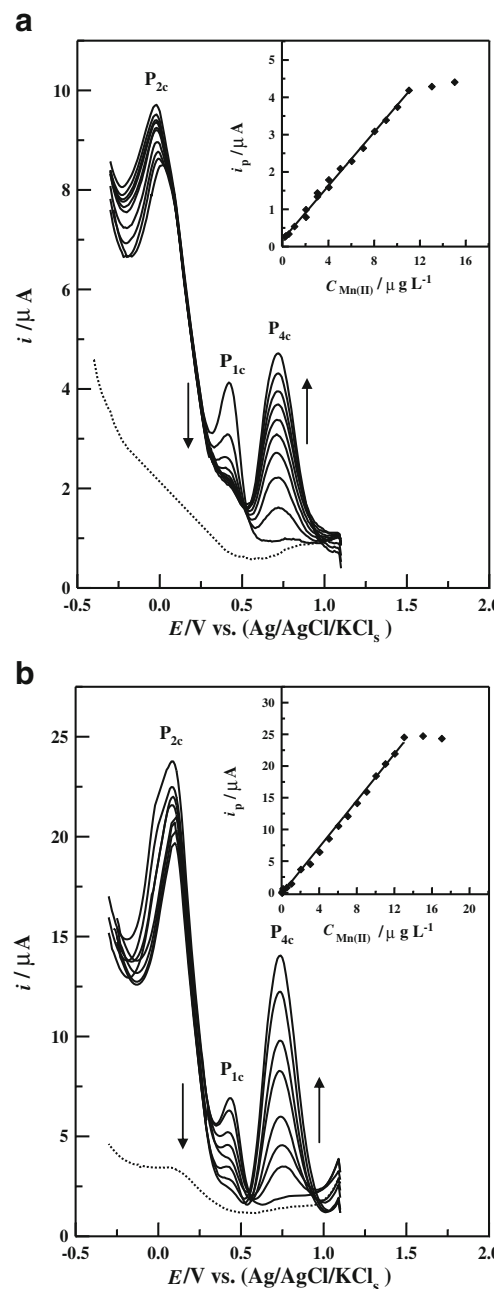


Fig. 8 SW-AdCS voltammograms recorded in the acetate buffer of pH 5 for $10 \mu\text{M}$ oxine and various concentrations of Mn(II): 0, 1, 2, 3, 4, 5, 6, 7, 8 and $9 \mu\text{g l}^{-1}$ Mn(II) using the bare CPE (a) and of 0, 1, 2, 3, 4, 5, 6 and $7 \mu\text{g l}^{-1}$ using the modified CPE (b) following preconcentration by adsorptive accumulation for 250 s at +1.1 V. Dotted line represents the blank solution ($f=80 \text{ Hz}$, $\Delta E_s=10 \text{ mV}$ and $E_a=25 \text{ mV}$). Insets: plots of i_p as a function of concentration of Mn(II)

parameters: $f=80 \text{ Hz}$, $\Delta E_s=10 \text{ mV}$ and $a=25 \text{ mV}$, which were used in the rest of this study.

Effect of preconcentration parameters

In the SW-AdCSV method, the preconcentration (accumulation) potential (E_{acc}) applied on the working electrode affects the

efficiency of the adsorption of the analyte species as a result of coulombic effects and competitive adsorption [52]. Thus, the effect of varying the applied accumulation potential between +1.3 and +1.0 V (vs. Ag/AgCl/KCl_s) on the peak current magnitude of the SW-AdCS voltammograms of 20 µg l⁻¹ of Mn(II) in the acetate buffer solution of pH 5 in the presence of 10 µM oxine was evaluated, following preconcentration onto the surface of both bare CPE and modified CPE, for 50 s (Fig. 7a, curves a and b, respectively). A much better enhanced peak current magnitude was achieved at +1.1 V. This is attributed to the increase of accumulation rate due to the more favorable alignment of the molecules by the electric field at the electrode solution interface [53]. The observed gradual decrease in peak current magnitude around the potential of +1.1 V may be the consequence of desorption of Mn(II)-oxine complex at much higher or lower potential in comparison to the potential zero charge [54]. Hence, an accumulation potential of +1.1 V was chosen for the rest of this analytical study.

On the other hand, the dependence of SW-AdCSV peak current magnitudes of 5 and 20 µg l⁻¹ of Mn(II) in the presence of 10 µM oxine on the preconcentration (accumulation) time (*t*_{acc}) at +1.1 V was examined using both bare CPE and modified CPE (Fig. 7b). The longer the accumulation time, the more the Mn(II)-oxine complex is adsorbed, and consequently the peak current magnitude increased. For 20 µg l⁻¹ of Mn(II), the response was linear up to about 90 s using the bare CPE and the modified CPE, leveled off, then decreased (Fig. 7b, curve a, and the inset, respectively). This indicates that the adsorptive equilibrium onto both bare CPE and modified CPE surface was achieved [54] (i.e., full surface coverage was approached). Thus, when saturation of the electrode surface was reached, the interactions among the molecules in the adsorbed state become noticeable, and the peak current magnitude started to decrease at longer accumulation times (i.e., desorption phenomena). For determination of the lowest Mn(II) concentrations, an extension of accumulation time is recommended. For 5 µg l⁻¹ of Mn(II), as the preconcentration time was increased, linearity

prevailed over the tested preconcentration time using both bare CPE and modified CPE (Fig. 7b, curve b). Thus, the preconcentration time of choice will be dictated by the sensitivity needed. In the present analytical investigations, the preconcentration time of 250 s only was applied because when accumulation time is higher than 250 s, the baseline will no longer be optimal.

Accordingly, the optimal operational conditions of the described SW-AdCSV method were as follows: *E*_{acc}=+1.1 V, *t*_{acc}=250 s, *f*=80 Hz, Δ*E*_s=10 mV, *a*=25 mV and 0.1 mol L⁻¹ sodium acetate buffer of pH 5 as the supporting electrolyte.

Method validation

Linearity range

Under the optimized conditions, SW-AdCS voltammograms of various concentrations of Mn(II) in the presence of 10 µM oxine were recorded following preconcentration by adsorptive accumulation of Mn(II)-oxine complex onto both the bare CPE and the modified CPE with 7 % (w/w) MMT-Na clay at +1.1 V for 250 s (Fig. 8a and b, respectively). It is clear that, upon the increase of Mn(II) concentration, the peak current magnitude of the Mn(II)-oxine complex (P_{4c}) increased at the expense of that of the first peak (P_{1c}) of the free neutral oxine (basic form; HL) rather than that of the second peak (P_{2c}) of free cationic oxine (acidic form: H₂L⁺), indicating again the formation of neutral Mn(II)-oxine complex (Scheme 2). Furthermore, the peak current magnitudes (*i*_p) of peak P_{4c} versus concentrations (*C*) of the Mn(II) at both the bare CPE and the modified CPE were straight lines within the concentration ranges 0.15–11 and 0.006–13 µg l⁻¹ Mn(II), respectively. At higher concentrations, the curves leveled off; this may be due to the saturation of the surface of the two CP electrodes (inset of Fig. 8a and b). The corresponding regression equations of the two curves were:

$$i_p(\mu\text{A}) = 0.355 \pm 4.2 \times 10^{-3} C(\mu\text{g l}^{-1}) + 0.25 \pm 5.3 \times 10^{-3} \quad (\text{at bare CPE}) \\ (r = 0.997 \text{ and } n = 14)$$

$$i_p(\mu\text{A}) = 1.84 \pm 2.5 \times 10^{-3} C(\mu\text{g l}^{-1}) - 0.22 \pm 1.1 \times 10^{-3} \quad (\text{at modified CPE}) \\ (r = 0.998 \text{ and } n = 19)$$

It is noticed that the shape of the two curves is practically the same as the shape of the adsorption curve derived from the Langmuir type isotherm of adsorption [55], and this fact can be regarded as supporting evidence to the monomolecular layer adsorption of the complexed species on the surface of CP electrodes. LOD and limit of quantitation (LOQ) of Mn(II)

were estimated using the expressions [56]: LOD=3 SD/b and LOQ=10 SD/b, where SD is the standard deviation of the replicate blank responses (or the intercept of the calibration plot) and *b* is the slope of the regression equation. LOD of 0.045 µg l⁻¹ (8.19×10⁻¹⁰ mol L⁻¹) and 0.0018 µg l⁻¹ (3.28×10⁻¹¹ mol L⁻¹) Mn(II) and LOQ of 0.15 µg l⁻¹

$(2.73 \times 10^{-9} \text{ mol L}^{-1})$ and $0.006 \mu\text{g L}^{-1}$ ($1.09 \times 10^{-10} \text{ mol L}^{-1}$) Mn(II) were achieved by the optimized SW-AdCSV method using the bare CPE and the modified CPE, respectively.

The results indicated the reliability of the optimized SW-AdCSV method for trace assay of Mn(II) at both electrodes. However, the achieved LOD of Mn(II) using the modified CPE is much more sensitive than all those reported in the literature [5–33, 35–42] using various electrode materials; however, it is fairly comparable with that obtained with DP CSV using boron-doped diamond electrode only ($\text{LOD}=1.0 \times 10^{-11} \text{ mol L}^{-1}$) [34] (Table 1).

Repeatability and reproducibility

Repeatability and reproducibility (expressed as % recovery, precision and accuracy) [57] of the described SW-AdCSV method were evaluated by performing five replicate measurements for various concentrations of Mn(II) ($1\text{--}9 \mu\text{g L}^{-1}$ in the presence of $10 \mu\text{M}$ of oxine) over 1 day (intra-day assay) and for successive 3 days (inter-day assay), following preconcentration by adsorptive accumulation onto both bare CPE and modified CPE at $+1.1 \text{ V}$ for 250 s. The results obtained by the described methods are summarized in Table 2. Insignificant differences were observed between the concentration of Mn(II) taken and found. Satisfactory mean recoveries, relative standard deviations and relative errors were achieved, indicating the repeatability, reproducibility, precision and accuracy of the described method for assay of Mn(II).

Robustness

The robustness [57] of the developed stripping voltammetric method was examined by studying the effect of variation of

some of the effective operational conditions such as pH (4.5 to 5.5), preconcentration potential ($+1.05$ to $+1.15 \text{ V}$) and preconcentration time (245 to 255 s). The obtained mean percentage recoveries and relative standard deviations ($\%R \pm \text{RSD}$) based on five replicate measurements under the varied conditions were 97.9 ± 0.9 to 98.3 ± 1.5 . Since the mean percentage recoveries and relative standard deviations obtained under the varied operational conditions were not significantly affected, the developed SW-AdCSV method is reliable for quantization of Mn(II) as Mn(II)-oxine complex and could be considered robust.

The inter-laboratory precision

The inter-laboratory precision [57] was also examined for analysis of different concentrations of Mn(II) ($5\text{--}10 \mu\text{g L}^{-1}$ Mn(II) in the presence of $10 \mu\text{M}$ of oxine) by means of the described SW-AdCSV method using two Potentiostats PAR-263A (Lab 1) and PAR-273 (Lab 2) at different elapsed times by two different analysts. The obtained mean recoveries and relative standard deviations (98.2 ± 2.2 to 98.7 ± 2.7) were found reproducible.

Selectivity

To check the selectivity of the described stripping voltammetric method, the influence of many ions (which are of great significance in environmental matrices) on the determination of Mn(II) was examined. Interference was taken as the level causing an error on the stripping voltammetric peak current magnitude of Mn(II)-oxine complex of 5 %. The results of this study are summarized in Table 3. The cations and the anions concentrations up to the tolerance level ($\approx 95\%$ to

Table 2 Representative results of intra-day and inter-day assays of various concentrations of Mn(II) by means of the described SW-AdCSV method using both the bare and modified CP electrodes ($n=5$)

$C_{\text{Taken}} (\mu\text{g L}^{-1})$	Intra-day				Inter-day			
	Mean C_{Found} ($\mu\text{g L}^{-1}$)	Mean recovery %R	Precision RSD%	Accuracy RE%	Mean C_{Found} ($\mu\text{g L}^{-1}$)	Mean recovery %R	Precision RSD%	Accuracy RE%
Utilizing the bare CPE								
1	0.99	99.0	1.0	-1.0	0.97	97.4	0.9	-2.6
3	3.05	101.7	0.7	1.7	2.93	97.7	1.1	-2.3
6	5.89	98.2	1.0	-1.8	5.88	98.0	2.1	-2.0
9	9.08	100.9	1.2	0.9	8.88	98.7	1.9	-1.3
Utilizing the modified CPE with 7 % (w/w) MMT-Na clay								
1	0.99	99.3	1.1	-0.7	0.98	98.0	0.9	-2.0
3	2.96	98.7	1.3	-1.3	3.08	102.7	1.3	2.7
6	6.03	100.5	1.5	0.5	6.05	100.8	2.3	0.8
9	8.85	98.3	2.2	-1.7	8.84	98.2	2.5	-1.8

n denotes the number of replicate determinations

Table 3 Interferences of some inorganic species in determination of 0.01 mg l^{-1} Mn(II) as Mn(II)-oxine complex by the described SW-AdCSV method using both the bare and the modified CP electrodes

Foreign species	Tolerance level ^a (mg l^{-1})	
	Bare CPE	Modified CPE
Cl^- , NO_3^- ,	9.8	10.0
SO_4^{2-} , PO_4^{3-} ,	5.3	5.0
HCO_3^- ,	4.0	3.5
K^+ , Na^+ ,	10.0	10.5
Mg^{2+} , Ca^{2+} , Bi^{3+} , Sb^{3+} , Se^{4+}	7.0	8.0
Ni^{2+} , Al^{3+}	3.5	3.0
Cd^{2+} , Cu^{2+} , Zn^{2+} , Co^{2+} , Pb^{2+} , Fe^{3+}	0.95	1.0

^a For 5 % error

1,000-fold) changed the signals of 0.01 mg l^{-1} Mn(II) by only 5 % at the maximum (Table 3). From these results, it can be concluded that the method is free from interferences of most of these foreign ions up to very high levels, i.e., these ions do not compete with Mn(II) for complexation with the oxine and for adsorption onto the CP electrodes within their potential range in contrast to the previous work using BDD electrode [34] which suffers from interference of Al(III), Fe(II) and Hg(II) in determination of Mn(II).

Interferences

The interferences of some natural organics were investigated in a typical way by the addition of non-ionic surfactant (Triton X-100) and humic acid (which is a subclass of humic substances present in natural waters in concentrations ranging from 0.02 mg l^{-1} in ground waters up to 30 mg l^{-1} in surface waters [58]). The presence of carboxylate and phenolate groups gives humic acid the ability to form complexes with several ions. Insignificant interference was obtained in the presence of Triton X-100 up to 0.001 %. However, a higher concentration of the surfactant caused a strong deformation

Table 5 Determination of Mn(II) as Mn(II)-oxine complex in various seawater samples by the described SW-AdCSV using the bare and the modified CP electrodes ($n=5$)

Sample	C_{added} ($\mu\text{g l}^{-1}$)	Bare CPE		Modified CPE	
		$C_{\text{found}}^{\text{a}}$ ($\mu\text{g l}^{-1}$)	%R±RSD	$C_{\text{found}}^{\text{a}}$ ($\mu\text{g l}^{-1}$)	%R±RSD
1	0.0	4.30	—	4.03	—
	2.0	6.29	99.5 ± 1.0	6.03	100.0 ± 1.0
	4.0	8.22	98.0 ± 1.3	8.00	99.3 ± 1.1
	6.0	10.28	99.7 ± 1.3	10.14	101.8 ± 0.9
	2	4.50	—	4.20	—
	2.0	6.47	98.5 ± 0.8	6.18	99.0 ± 0.9
3	4.0	8.43	98.3 ± 1.2	8.15	98.8 ± 1.1
	6.0	10.50	100.3 ± 1.3	10.11	98.5 ± 1.2
	0.0	4.40	—	3.90	—
	2.0	6.45	102.5 ± 1.5	5.94	102.0 ± 1.0
	4.0	8.49	102.3 ± 1.0	7.92	100.5 ± 1.2
	6.0	10.50	101.7 ± 1.4	9.95	100.8 ± 1.3

^a Mean values of five replicate determinations

and suppression of the Mn(II)-oxine complex's voltammetric peak, making the determination of Mn(II) impossible. The influence of surfactants in seawater can be completely eliminated through mineralization of the water samples prior to the analysis. However, the presence of surfactants in tap and bottled natural water is unexpected. Also, a 300-fold excess of humic acid had no influence on the determination of 0.01 mg l^{-1} Mn(II); however, at higher concentrations of humic acid, a decrease in the analytical response of Mn(II) was observed due to competition of this ligand in complex formation of Mn(II). The total amount of dissolved organic matters in the open seawater usually did not exceed 2 mg l^{-1} and the concentration of humic acid is less than 0.11 mg l^{-1} [59]; therefore, no noticeable interference may be expected in open seawater analysis. However, preliminary UV digestion

Table 4 Determination of Mn(II) as Mn(II)-oxine complex in various environmental water samples by the described SW-AdCSV method using both the bare and the modified CP electrodes

Analyzed sample	$C_{\text{found}}^{\text{a}}$ ($\mu\text{g l}^{-1}$) Bare CPE	%R±RSD	$C_{\text{found}}^{\text{a}}$ ($\mu\text{g l}^{-1}$) Modified CPE	%R±RSD
Ground water	640.64	98.9 ± 2.2	633.56	99.0 ± 1.6
Tap water	130.55	99.2 ± 1.5	128.68	98.9 ± 2.0
Bottled water				
Delta	30.59	100.0 ± 0.9	28.88	100.5 ± 1.3
Aquafina	13.18	99.6 ± 1.3	13.09	99.3 ± 2.0
Siwa	8.34	99.9 ± 1.0	8.80	101.4 ± 1.2
Safi	6.17	101.1 ± 1.0	5.59	100.6 ± 1.6
Nestle	5.80	98.9 ± 2.0	6.05	100.1 ± 1.6

^a Mean values of five replicate determinations

of seawater and the standard additions method are used in this work.

Applications

Various water samples (ground water, tap water, bottled natural water and coastal seawater) were analyzed for their Mn(II) contents by the described SW-AdCSV method using both the bare CPE and the modified CPE. The seawater samples were first digested by UV irradiation in the presence of HCl (pH 1) for 30 min before analysis to destroy organic matter. The calibration curve method was used for estimating the concentration of Mn(II) in the analyzed water samples. However, the standard addition method was also applied for three different standard Mn(II) solutions added to a pre-analyzed solution of the investigated water sample in order to minimize the sample matrix interference. Typical analytical results corresponding to the mean values of five replicate determinations are summarized in Tables 4 and 5. Satisfactory mean percentage recoveries (%R) and precision (RSD%) for determination of Mn(II) in various water samples were obtained using both the calibration curve and the standard addition methods (e.g., Tables 4 and 5).

Moreover, depending on the possibility that these real water samples may contain several other metal ions, higher oxine concentrations (15–35 µM) were also tested to ensure complete Mn(II)–oxine complex formation. Insignificant difference in the mean concentration found, %R and RSD% were obtained, indicating that optimized oxine concentration is sufficient enough for the formation of complex with Mn(II) in the investigated water samples.

Conclusion

In this study, oxine is described, for the first time, as an efficient and selective ligand for electrochemical trace determination of Mn(II). A validated adsorptive CSV method coupled with both bare CPE and modified CPE with 7 % (w/w) MMT-Na clay was used. The described stripping voltammetry method is simple, selective and sensitive. The achieved LOD of Mn(II) as oxine–complex are much sensitive than those obtained using the voltammetric methods (using various electrode materials) reported in the literature [24–33, 35–43]. The proposed method was applied for the determination of Mn(II) in various environmental water samples without interference from various organic and inorganic species.

References

- Siegel A, Siegel H (2000) Metal ions in biological systems: manganese and its role in biological processes. CRC Press, Boca Raton
- Michalke B (2004) J Chromatogr A 1050:69–76
- Gerber GB, Leonard A, Hantson P (2002) Crit Rev Oncol Hematol 42:25–34
- Pearson GF, Greenway GM (2005) Trends Anal Chem 24:803–809
- Tang B, Han F (2001) Anal Lett 34:1353–1368
- Klamtet J (2006) Nu Sci J 2:165–173
- Kumar AP, Reddy PR, Reddy VK (2009) Eurasian J Anal Chem 4:66–75
- Abbas-Tarighat M, Shahbazi E, Niknam K (2013) Food Chem 138:991–997
- Su L, Li JG, Ma HB, Tao GH (2004) Anal Chim Acta 522:281–288
- Pourreza N, Kamran-HeKani S, Rastegarzadeh S (1998) Can J Anal Sci Spectr 43:149–152
- Pohl P, Sergiel I (2010) Microchim Acta 168:9–15
- Truuus K, Viitak A, Vaher M, Muinasmaa U, Paasrand K, Tuvikene R, Levandi T (2007) Proc Estonian Acad Sci Chem 56:122–133
- Anjos AP, Ponce LC, Cadore S, Baccan N (2007) Talanta 71:1252–1256
- Mohan AM, Mandakolathur SS (2003) J AOAC Int 86:1218–1224
- Korn MA, -de Freitas Santos AJ, Jaeger HV, Silva NMS, Spínola Costa AC (2004) J Braz Chem Soc 15:212–218
- Cesur H (2003) Turk J Chem 27:307–314
- Milne A, Landing W, Bizimis M, Morton P (2010) Anal Chim Acta 665(2010):200–207
- Chen S, Xiao M, Lu D, Wang Z (2007) Spectrochim Acta Part B 62:1216–1221
- Hasegawa S, Kobayashi T, Hasegawa R (2000) Mater Trans JIM 41:841–845
- Sohrin Y, Urushihara S, Nakatsuka S, Kono T, Higo E, Minami T, Norisuye K, Umetani S (2008) Anal Chem 80:6267–6273
- Welz B, Sperling M (1999) Atomic absorption spectrometry, 3rd edn. VCH, Weinheim
- Gupta VK, Jain R, Pal MK (2010) Int J Electrochem Sci 5:1164–1178
- Gholivand MB, Gorji M, Josaghani M (2009) Collect Czech Chem Commun 74:1411–1424
- Colombini MP, Fuoco R (1983) Talanta 30:901–905
- Radhi MM, Tan WT, Ab Rahman MZB, Kassim AB (2010) Int J Electrochem Sci 5:254–266
- Ching YM, Tee TW, Zainal Z (2011) Int J Electrochem Sci 6:5305–5313
- Rezaei B, Ghiaci M, Sedaghat ME (2008) Sensors Actuators B 131:439–447
- Piech R, Baś B, Kubiak WW (2008) J Electroanal Chem 621:43–48
- Ghoneim MM, Hassanein AM, Hammam E, Beltagi AM (2000) Fresenius J Anal Chem 367:378–383
- Locatelli C, Torsi G (2001) J Electroanal Chem 509:80–89
- Yue W, Bange A, Riehl BL, Riehl BD, Johnson JM, Papautsky I, Heineman WR (2012) Electroanalysis 24:1909–1914
- Di J, Zhang F (2003) Talanta 60:31–36
- Jin J-Y, Xu F, Miwa T (2000) Electroanalysis 12:610–615
- Saterlay AJ, Foord JS, Compton RG (1999) Analyst 124:1791–1796
- Khoo SB, Soh MK, Cai Q, Khan MR, Guo SX (1997) Electroanalysis 9:45–51
- Stozhko NY, Inzhevskaya OV, Kolyadina LI, Lipunova GN (2005) J Anal Chem 60:163–168
- Filipe OMS, Brett CMA (2003) Talanta 61:643–650
- Rievaj M, Tomcik P, Janosikova Z, Bustin D, Compton RG (2008) Chem Anal 53:153–161
- Zhou J, Neeb R (1994) Fresenius J Anal Chem 350:593–598
- Wang J, Lu J (1995) Talanta 42:331–335
- El-Maali NA, El-Hady DA (1998) Anal Chim Acta 370:239–249

42. Ghoneim EM (2010) *Talanta* 15:646–652
43. Beltagi AM, Ismail IM, Ghoneim MM (2013) *Am J Anal Chem* 4:197–206
44. Korn MGA, Ferreira AC, Teixeira LSG, Costa ACS (1999) *J Braz Chem Soc* 10:46–50
45. Villalba MM, Davis J (2008) *J Solid State Electrochem* 12:1245–1254
46. Kamal MM, Ahmed SM, Shahata MM, Temerk YM (2002) *Anal Bioanal Chem* 372:843–848
47. Ramenskaya LM, Kraeva OV (2006) *Russ J Phys Chem* 80:90–94
48. Stević MC, Ignjatović LM, Ćirić-Marjanović G, Stanišić SM, Stanković DM, Zima J (2011) *Int J Electrochem Sci* 6:2509–2525
49. Patel KB, Kharadi GJ, Nimavat KS (2012) *J Chem Pharm Res* 4:2422–2428
50. Ujinaga T, Takagi O (1975) *Bull Inst Chem Res* 53:460–463
51. Devol I, Bardez E (1998) *J Colloid Interface Sci* 200:241–248
52. Campos MLAM, van den Berg CMG (1994) *Anal Chim Acta* 284:481–496
53. Yardım Y, Keskin E, Levent A, Ozsoz M, Senturk Z (2010) *Talanta* 80:1347–1355
54. Gupta VK, Jain R (2011) *Int J Electrochem Sci* 6:37–51
55. Jirgensons B, Starumans ME (1962) *Colloid chemistry*. Macmillan, New York
56. Miller JN (1991) *Analyst* 116:3–14
57. The United States Pharmacopeial Convention (2010) *The United States Pharmacopeia, USP 33-NF 28*, Rockville, MD
58. Brum MC, Oliveira JF (2007) *Miner Eng* 20:945–949
59. Wang CS, Boyle E, Bruland KW, Burton JD, Goldberg ED (1983) *Trace metals in sea water*. Plenum, London